Research Article

Barrier Properties and Structural Study of Nanocomposite of HDPE/Montmorillonite Modified with Polyvinylalcohol

María C. Carrera,[1] Eleonora Erdmann,[2] and Hugo A. Destéfanis[1]

[1] *Instituto de Investigaciones para la Industria Química (INIQUI-CONICET), Consejo de Investigaciones (CIUNSa), Facultad de Ingeniería (UNSa), Avenida Bolivia 5150, 4400 Salta, Argentina*

[2] *Instituto Tecnológico de Buenos Aires (ITBA), Instituto de Investigaciones para la Industria Química (INIQUI-UNSa-CONICET), Avenida Eduardo Madero 399, C1106ACD Buenos Aires, Argentina*

Correspondence should be addressed to María C. Carrera; celestecarrera@gmail.com

In this work was studied the permeation of CO_2 in films of high-density polyethylene (HDPE) and organoclay modified with polyvinylalcohol ($MMT_{HDTMA/PVA}$) obtained from melt blending. Permeation study showed that the incorporation of the modified organoclay generates a significant effect on the barrier properties of HDPE. When a load of 2 wt% of $MMT_{HDTMA/PVA}$ was incorporated in the polymer matrix, the flow of CO_2 decreased 43.7% compared to pure polyethylene. The results of TEM showed that clay layers were dispersed in the polymeric matrix, obtaining an exfoliated-structure nanocomposite. The thermal stability of nanocomposite was significantly enhanced with respect to the pristine HDPE. DSC results showed that the crystallinity was maintained as the pure polymeric matrix. Consequently, the decrease of permeability was attributable only to the effect of tortuosity generated by the dispersion of $MMT_{HDTMA/PVA}$. Notably the mechanical properties remain equal to those of pure polyethylene, but with an increase in barrier properties to CO_2. This procedure allows obtaining nanocomposites of HDPE with a good barrier property to CO_2 which would make it competitive in the use of packaging.

1. Introduction

The barrier properties of polymers can be significantly altered by inclusion of impermeable lamellar fillers such as montmorillonites, with sufficient aspect ratio to alter the diffusion path of gas-penetrant molecules. The key issue is to obtain an effective dispersion and exfoliation of the platelets into the polymer matrix to yield a tortuous diffusion pathway for improved barrier properties. In most works concerning nanocomposites, the barrier properties are examined by using gas [1–5] and the literature contains numerous reports on decreased gas permeability [6–20] caused by addition of layered silicates to various polymer matrices.

Enough articles in the literature have focused the studies on nanocomposites made by addition of organoclays, formed from montmorillonite, to thermoplastics using melt-processing techniques [6, 7, 21–26]. This method involves the mixing of the layered silicate with the polymer and heating the mixture above its softening point. Under certain conditions, if the clay layer surfaces are sufficiently compatible with the polymer chains, the polymer can enter between the interlayer spaces, forming an intercalated or exfoliated nanocomposite [27–29]. The incorporation of small amounts (<10 wt%) of clay shows a remarkable influence on the permeability and barrier properties of composite membranes [30].

In the preparation of polymer/clay nanocomposites, is very important the chemical interaction between polymer and clay. For instance, in the case of polyamides and some types of clay, the surface forces are very large due to hydrogen-bond-type interactions; in this case exfoliation is not a difficult process. Nevertheless, in the case of nonpolar polymers like high-density polyethylene (HDPE), there is no good interaction between hydrophilic clays and polymer and the adhesion between them is very poor, resulting in final materials with mechanical and rheological properties well below the pristine polyethylene [31].

To improve the interaction with hydrophobic polymers such as HDPE, the clay is organophilized, increasing polymer/clay affinity and the ability of forming exfoliated nanocomposites [32, 33].

In this work nanocomposites of HDPE and modified clay were prepared by melt blending. The modified clay was obtained in two stages. In the first step the clay was exchanged with hexadecyltrimethylammonium (MMT_{HDTMA}) and in the second step the MMT_{HDTMA} was modified with polyvinyl alcohol (PVA) by in situ polymerization ($MMT_{HDTMA/PVA}$).

In this work was studied the influence of the organoclay modified with PVA on the structure and barrier properties to CO_2 of the nanocomposites. The control CO_2 permeability is of fundamental importance in the selection of materials for food packaging under modified atmosphere (MA), whose principle is to achieve an environment with low concentration of O_2 and high concentration of CO_2 inside the package [34]. Consequently the reduction of CO_2 permeability allows the use of HDPE as a packaging material for many food products. Moreover, the hydrophilic properties of the nanocomposite material make it suitable for use in gas lines, tanks, and pipelines for hydrocarbons [35].

X-ray diffraction (XRD), scanning electron microscopy (SEM), and transmission electron microscopy (TEM) were used to observe the internal structure and morphology of the nanocomposite obtained. The heat stability was studied by thermogravimetric analysis (TGA) and differential scanning calorimetry (DSC).

2. Experimental

2.1. Materials. An HDPE, 40055L from Polisur S.A, with melt flow index of 10 g/10 min (290°C, 21.6 kg) was chosen as a matrix.

Sodium montmorillonite (MMT) clay supplied by Minarmco (CEC = 70 meq/100 g and particle size < 325 mesh), was organically modified with a hexadecyltrimethylammonium bromide salt (MERCK) (HDTMA) following the modified technique of Yeh et al. [33]. The organophilic clay was modified by in situ polymerization: the vinyl acetate monomer (vinyl acetate (VETEC, Brazil)) was intercalated into layer of MMT_{HDTMA} and followed by a free radical polymerization with benzoyl peroxide as an initiator reaction. The polyvinyl acetate/MMT_{HDTMA} solution was saponified by alcoholysis with NaOH solution to obtain polyvinyl alcohol-modified organophilic clay ($MMT_{HDTMA/PVA}$) [36].

2.2. Melt Mixing. Nanocomposites of HDPE with loads of 0.6 wt% and 2 wt% of organoclay modified with PVA were prepared using a mixing chamber Rheomix 600 coupled to a Haake Rheocord 9000 torque rheometer with roller type rotors. The temperature used was 190°C and the speed of work was 90 rpm.

2.3. Characterization. Films for characterization were prepared by compression molding of the nanocomposites using a Carver model hydraulic press, under 27.6 MPa pressure at 190°C for 5 minutes.

X-ray diffraction (XRD) analyses were performed in a Rigaku Miniflex DRX 600 diffractometer using nickel-filtered $CuK\alpha$ radiation operating at 30 kV and 15 mA. The data were recorded at 2θ rate of $2°min^{-1}$.

Scanning electron microscopy (SEM) was carried out using a JEOL JSM-6480 LV microscope with an accelerating voltage of 15 kV. Samples were coated with gold in order to study the surface morphology.

The sample for TEM was cut from cry oultramicrotome, RMC Powertome XL at 60 nm thickness with diamond knife at a temperature of −40°C. The sections were transferred into a copper grid. TEM imaging was done using Jeol JEM 2000FX electronic microscope operating at 200 kV accelerating voltage.

2.4. Measurement of Properties. The thermal behavior was carried out using a TA Instrument TGA model Q500 from 30°C to 700°C with a heating rate of $10°C·min^{-1}$, operating under N_2 flow of 60 mL·min^{-1}. The melting point and fusion enthalpy were obtained by differential scanning calorimeter, DSC, model Q100, TA Instrument. Samples were heated from 20°C to 200°C at a rate of $10°C·min^{-1}$ then cooled down to 20°C and heated again at the same rate to 250°C under N_2 atmosphere. The crystallinity data were obtained from the second heating run.

The CO_2 permeation was carried out in an equipment of permeation standard (Permatran C200), at a temperature of 26°C and humidity of 0%. The concentration of CO_2 used was 100% in films of 0.2 mm thickness.

Tensile tests were carried out on seven films of each sample, for using an instron tensile testing machine model 5569 at 23°C and 45% relative humidity, following the ASTM-D882 method. The test was performed at 10 mm/min of strain speed.

3. Results and Discussion

3.1. Morphology and Internal Structure. Figure 1(a) shows XRD of unmodified organoclay (MMT_{HDTMA}), clay modified with PVA ($MMT_{HDTMA/PVA}$), and the modified clay mixed with HDPE 2 wt%. The peak at low angle of 4.6 degree in Figure 1(a) corresponds to the basal reflection (001) of the organoclay (MMT_{HDTMA}). The diffractogram of the sample of $MMT_{HDTMA/PVA}$ shows a disappearance of the peaks between $2\theta = 2°–10°$, which would indicate a possible exfoliation, since the PVA chains could have destroyed completely the ordered structure of the clay. In the HDPE/$MMT_{HDTMA/PVA}$ material, with load of 0.6 wt% and 2 wt% (Figure 1(b)) the diffraction peaks were not observed between 2–5 degree, in the XRD diffractograms, either because of a much too large spacing between the layers (i.e., exceeding 8 nm in the case of ordered exfoliated structure) or because the nanocomposite does not present ordering anymore [27].

Figure 2(a) shows the SEM micrograph of the typical morphology of a binary mixture of HDPE and PVA which are incompatible polymers. It shows large PVA particles with poor interfacial adhesion and dispersion in the polyethylene
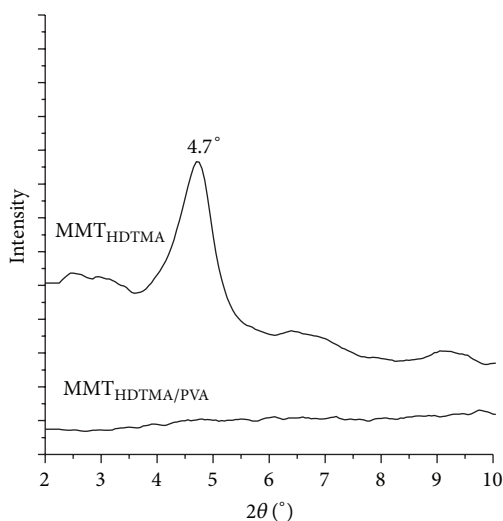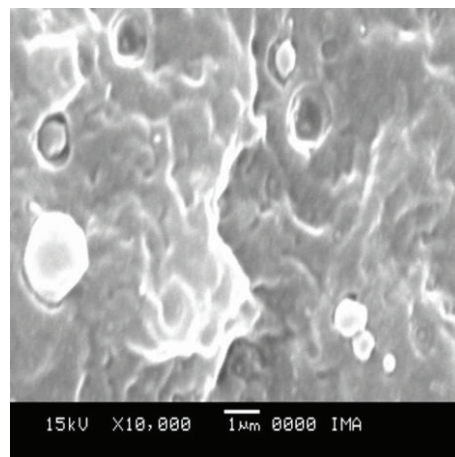
(a)
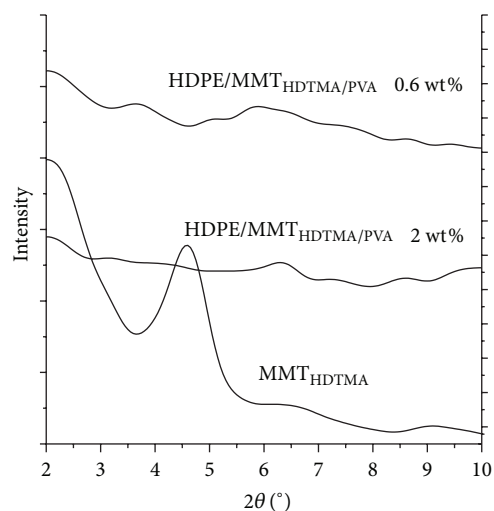
(b)

Figure 1: X-ray diffraction curves of (a) MMT_{HDTMA} and $MMT_{HDTMA/PVA}$ and (b) MMT_{HDTMA} and HDPE/$MMT_{HDTMA/PVA}$ with 0.6 wt% and 2 wt%.

(a)

(b)

Figure 2: SEM (a) images of HDPE/$MMT_{HDTMA/PVA}$ with 0.6 wt% (a) and 2 wt% (b).
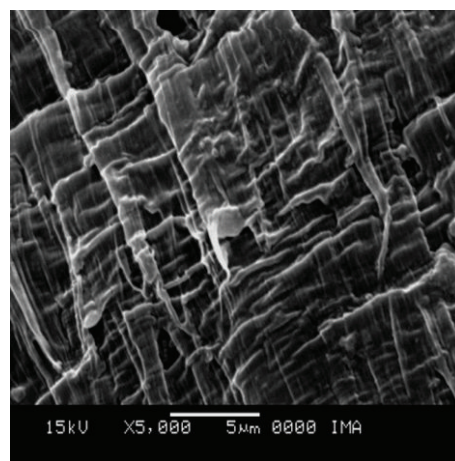
matrix. The morphology improves when the load organoclay was increased in the polymer matrix (Figure 2(b)), especially when the loads were high (2 wt%), meaning that, a good dispersion of the clay was obtained in the polymeric matrix.

The TEM image in Figure 3 shows completely different structures having two different loads of $MMT_{HDTMA/PVA}$ in the polymer matrix of polyethylene. When the load is 0.6 wt% the presence of two types of structures (agglomerate) and alternating layers (intercalated) is observed (Figures 3(a)–3(c)). While the XRD of this material (HDPE/$MMT_{HDTMA/PVA}$) was not observed any peak could be the low concentration of clay in the polymer matrix that is not detected by the team and not as previously thought exfoliation in when those results (XRD).

When the load of clay is 2 wt% the material presents an exfoliated structure (Figures 3(d)–3(f)) which is consistent with XRD results (Figure 1(b)).

3.2. Thermal Behavior and Crystallinity.
Figure 4 shows that, in general terms, in the thermal stability of the HDPE composite materials obtained by TGA only a small change has occurred. The presence of $MMT_{HDTMA/PVA}$ causes a change in the profile of DTGA (Figure 4), because was observed decomposition processes PVA (dehydration: 200°C–400°C) and ammonium salt which occur in the same range.

DSC results of HDPE and HDPE/$MMT_{HDTMA/PVA}$ nanocomposite are shown in Figure 5. The melting point (T_m) of the nanocomposites does not change with regard to pristine HDPE.

The polymers are semicrystalline materials, where crystalline regions are surrounded by amorphous regions, so the properties are influenced by the degree of crystallinity and the size and shape of the crystals. The degree of crystallinity of the samples was calculated using the total enthalpy method [38] from (1), taking the data of enthalpy of fusion of each material (ΔH_m), obtained from the area under the curve of heat versus temperature, Figure 5.

$$\chi_C = \frac{\Delta H_m}{\Delta H_m^0}, \tag{1}$$

(a)   (b)   (c)

(d)   (e)   (f)
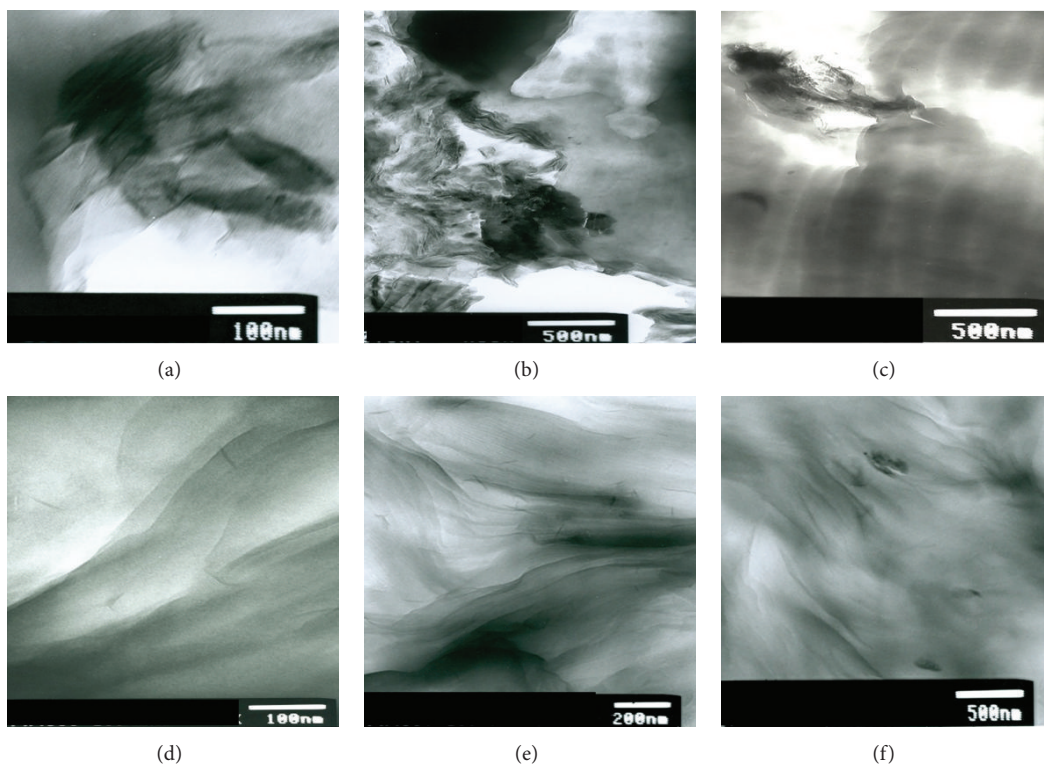
FIGURE 3: TEM images of HDPE/MMT$_{HDTMA/PVA}$ with 0.6 wt% (X100 (a), X500 (b), and X500 (c)) and 2 wt% (X100 (d), X200 (e), and X500 (f)).
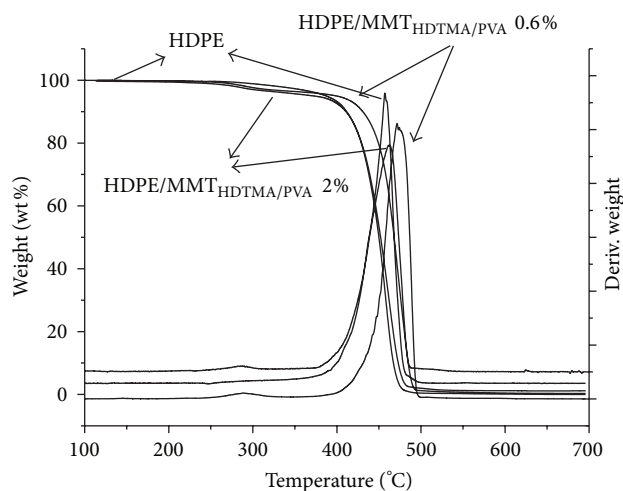

FIGURE 4: TG and DTG curves of HDPE, HDPE/MMT$_{HDTMA/PVA}$ 0.6 wt%, and HDPE/MMT$_{HDTMA/PVA}$ 2 wt%.
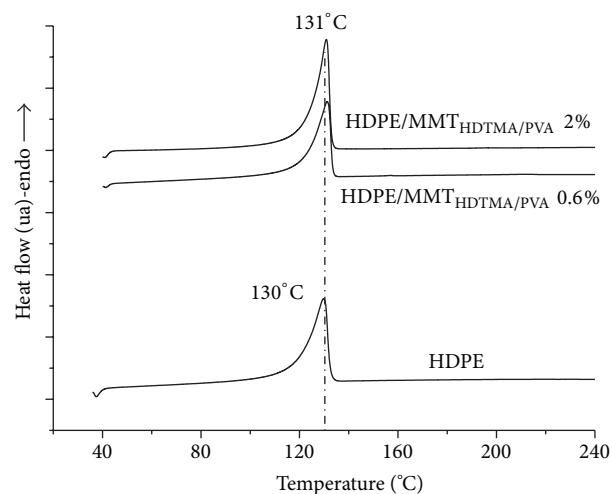
FIGURE 5: DSC curves of HDPE, HDPE/MMT$_{HDTMA/PVA}$ 0.6 wt%, and HDPE/MMT$_{HDTMA/PVA}$ 2 wt%.

where ΔH_m^0 is the crystalline fusion enthalpy to 100% crystalline polyethylene ($\Delta H_m^0 = 288$ J·g^{-1} [38]) and ΔH_m is the material fusion enthalpy.

In terms of the crystallinity of the composite materials shown in Table 1 it is not appreciably changed with respect to the original polymer.

TABLE 1: Fusion enthalpy and crystalline degree of the materials.

Sample	ΔH_m (J/g)	χ_C (%)
HDPE	156.1	54.2
HDPE/MMT$_{HDTMA/PVA}$ 0.6 wt%	131.8	50
HDPE/MMT$_{HDTMA/PVA}$ 2 wt%	142.0	49.3

TABLE 2: Mechanical properties of the materials.

Sample	Young's modulus (Mpa)	Yield stress (Mpa)	Yield elongation (%)	Tensile strength (Mpa)
HDPE	745 ± 88	12.1 ± 0.8	2.2 ± 0.4	20.4 ± 1.3
HDPE/MMT$_{\text{HDTMA/PVA}}$ (0.6 wt%)	657 ± 74	11.8 ± 0.5	2.3 ± 0.5	18.8 ± 1.8
HDPE/MMT$_{\text{HDTMA/PVA}}$ (2 wt%)	623 ± 45	13.9 ± 0.6	3.3 ± 0.6	21.2 ± 0.7

TABLE 3: CO_2 permeability of HDPE and HDPE/MMT$_{\text{HDTMA/PVA}}$ (0.6 wt% and 2 wt%).

Sample	P_{CO_2} (cm^3·mm/m^2·day)
HDPE	451 ± 22.4
HDPE/MMT$_{\text{HDTMA/PVA}}$ 0.6 wt%	553 ± 154
HDPE/MMT$_{\text{HDTMA/PVA}}$ 2 wt%	254 ± 25

3.3. Mechanical Properties. Tensile strength and elongations at yield point and at break of these nanocomposites are presented in Table 2. No significant change in these mechanical properties was observed when the modified clay was added to the HDPE.

3.4. Barrier Properties. Considering ideal gas behavior, the flow can be calculated according to (2) and the permeation by (3):

$$J = \frac{dV}{dt} \cdot \frac{1}{A}, \qquad (2)$$

$$P = J \cdot e, \qquad (3)$$

where A is the area of permeation, V is the volume of gas, t is the time to permeate, P is the permeation, and e is the thickness film.

The CO_2 permeability through the films of HDPE and the composite of HDPE with modified clay were obtained with the (3). Table 3 shows that the CO_2 permeability of material with 2 wt% organoclay modified with PVA decreases 43.7% compared to pure HDPE. With load of 0.6 wt% the permeability was increased 22.5% compared to pristine polyethylene. This behavior can be attributed to the fact that the main transport that controls the mechanism could be the interface polymer/clay and the films of HDPE/MMT$_{\text{HDTMA/PVA}}$ (0.6 wt%) with more defects at the interface have less resistance to permeation [39], that is, they do not have the sufficient amount of clay to increase the barrier properties.

The barrier properties were increased as a result of the tortuous path created by a 2 wt% of clay platelets [37]. This behavior can be attributed to a better orientation of the modified clay with an exfoliated structure to form a more tortuous path at the CO_2 diffusion in the membrane. On the other hand the main transport that controls the mechanism could be the interface polymer/clay.

From the results obtained a model was used to calculate the tortuosity. A simple permeability model for a regular arrangement of platelets has been proposed by Nielsen [10]
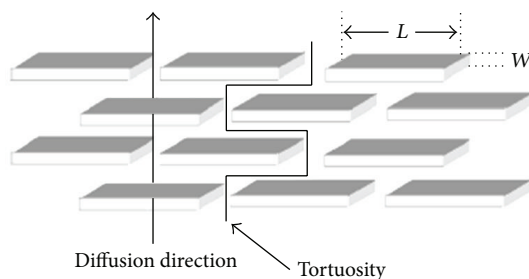

FIGURE 6: Regular arrangement of orthogonally shaped platelets in a parallel array with their main direction perpendicular to the diffusion direction (reproduced from [37]).

and is presented in Figure 6. The nanoparticles are evenly dispersed and considered to be rectangular platelets with finite width, L, and thickness, W. Their orientation is perpendicular to the diffusion direction [40].

The solubility coefficient of this nanocomposite is

$$S = S_0 \left(1 - \varphi\right), \qquad (4)$$

where S_0 is the solubility coefficient of the neat polymer and φ is the volume fraction of the nanoplatelets that are dispersed in the matrix. In this approximation the solubility does not depend on the morphological features of the phases.

The platelets act as impermeable barriers to the diffusing molecules, forcing them to follow longer and more tortuous paths in order to diffuse through the nanocomposite. The diffusion coefficient, D, is influenced by the tortuosity, τ:

$$D = \frac{D_0}{\tau}. \qquad (5)$$

Therefore a model for calculation of tortuosity is the following:

$$\tau = 1 + \frac{L}{2W}\varphi. \qquad (6)$$

Values of mean filler aspect ratio ($\alpha = L/W$) were calculated from a detailed analysis of several TEM images observed in Figures 3(a)–3(f). This values (α) and the tortuosity (τ) are observed in the Table 4.

The medium tortuosity for the nanocomposites with 0.6 wt% is $\tau_m = 1.15$ and 1.33 when the load of clay is 2 wt%. This explains that having substantial tortuosity the diffusivity of nanocomposite decreases with respect to the diffusivity of pure polyethylene and consequently decreases the permeability to CO_2 in the material with 2 wt%.

TABLE 4: Mean filler aspect ratio (α) and tortuosity of material of HDPE/MMT$_{HDTMA/PVA}$ (0.6 wt% and 2 wt%).

Sample	HDPE/MMT$_{HDTMA/PVA}$ 0.6 wt%			HDPE/MMT$_{HDTMA/PVA}$ 2 wt%		
Figure 3	(a)	(b)	(c)	(d)	(e)	(f)
$\alpha = L/W$	19	11	30	11	15	29
τ	1.14	1.10	1.20	1.20	1.27	1.51
τ_m		1.15			1.33	

4. Conclusion

The organoclay modified with PVA improved the CO_2 barrier properties of HDPE when the load is of 2 wt%, so it is very important to note the following surprising result for the nanocomposite: the flux density decreases about 43.7% as compared with pristine polyethylene. Since the crystallinity of the material is in the order of polyethylene, the decreased of CO_2 permeability is attributable solely to the incorporation of the organophilic clay-modified PVA, allowing a good dispersion of the plates in the polymer matrix. These results are consistent with the exfoliated structure of material obtained. Notably, the mechanical properties of the composite are maintained in the same order of polyethylene which makes it a competitive material with good mechanical properties which characterize the HDPE, but with barrier properties to CO_2 improved 43.7%.

References

[1] Z. Ke and B. Yongping, "Improve the gas barrier property of PET film with montmorillonite by in situ interlayer polymerization," *Materials Letters*, vol. 59, no. 27, pp. 3348–3351, 2005.

[2] O. Gain, E. Espuche, E. Pollet, M. Alexandre, and P. Dubois, "Gas barrier properties of poly(ε-caprolactone)/clay nanocomposites: influence of the morphology and polymer/clay interactions," *Journal of Polymer Science B*, vol. 43, no. 2, pp. 205–214, 2005.

[3] E. Picard, A. Vermogen, J. F. Gérard, and E. Espuche, "Barrier properties of nylon 6-montmorillonite nanocomposite membranes prepared by melt blending: influence of the clay content and dispersion state. Consequences on modelling," *Journal of Membrane Science*, vol. 292, no. 1-2, pp. 133–144, 2007.

[4] S. S. Ray, K. Yamada, M. Okamoto, A. Ogani, and K. Ueda, "New polylactide/layered silicate nanocomposites. 3. High-performance biodegradable materials," *Chemistry of Materials*, vol. 15, no. 7, pp. 1456–1465, 2003.

[5] T. Ogasawara, Y. Ishida, T. Aoki, and T. Ogura, "Helium gas permeability of montmorillonite/epoxy nanocomposites," *Composites A*, vol. 37, no. 12, pp. 2236–2240, 2006.

[6] S. S. Ray and M. Okamoto, "Polymer-layered silicate nanocomposite: a review from preparation to processing," *Progress in Polymer Science*, vol. 28, pp. 1539–1641, 2003.

[7] E. P. Giannelis, "Polymer-layered silicate nanocomposites: Synthesis, properties and applications," *The Applied Organometallic Chemistry*, vol. 12, pp. 675–680, 1998.

[8] E. P. Giannelis, "Polymer layered silicate nanocomposites," *Advanced Materials*, vol. 8, pp. 29–35, 1996.

[9] K. Yano, A. Usuki, and A. Okada, "Synthesis and properties of polyimide-clay hybrid films," *Journal of Polymer Science A*, vol. 35, no. 11, pp. 2289–2294, 1997.

[10] L. E. Nielsen, "Models for the permeability of filled polymers systems," *Journal of Macromolecular Science, Part A*, vol. 1, no. 5, pp. 929–942, 1967.

[11] N. K. Lape, E. E. Nuxoll, and E. L. Cussler, "Polydisperse flakes in barrier films," *Journal of Membrane Science*, vol. 29, pp. 29–37, 2004.

[12] D. Perry, W. J. Ward, and E. L. Cussler, "Unsteady diffusion in barrier membranes," *Journal of Membrane Science*, vol. 44, no. 2-3, pp. 305–311, 1989.

[13] N. K. Lape, C. Yang, and E. L. Cussler, "Flake-filled reactive membranes," *Journal of Membrane Science*, vol. 209, no. 1, pp. 271–282, 2002.

[14] C. Yang, W. H. Smyrl, and E. L. Cussler, "Flake alignment in composite coatings," *Journal of Membrane Science*, vol. 231, no. 1-2, pp. 1–12, 2004.

[15] W. R. Falla, M. Mulski, and E. L. Cussler, "Estimating diffusion through flake-filled membranes," *Journal of Membrane Science*, vol. 119, no. 1, pp. 129–138, 1996.

[16] R. K. Bharadwaj, "Modeling the barrier properties of polymer-layered silicate nanocomposites," *Macromolecules*, vol. 34, no. 26, pp. 9189–9192, 2001.

[17] A. A. Gusev and H. R. Lusti, "Rational design of nanocomposites for barrier applications," *Advanced Materials*, vol. 13, pp. 1641–1643, 2001.

[18] G. H. Fredrickson and J. Bicerano, "Barrier properties of oriented disk composites," *Journal of Chemical Physics*, vol. 110, pp. 2181–2188, 1999.

[19] S. S. Ray, K. Yamada, M. Okamoto, A. Ogami, and K. Ueda, "New polylactide/layered silicate nanocomposites. 3. High-performance biodegradable materials," *Chemistry of Materials*, vol. 15, no. 7, pp. 1456–1465, 2003.

[20] S. S. Ray, K. Okamoto, and M. Okamoto, "Structure-property relationship in biodegradable poly(butylene succinate)/layered silicate nanocomposites," *Macromolecules*, vol. 36, no. 7, pp. 2355–2367, 2003.

[21] H. R. Dennis, D. L. Hunter, D. Chang et al., "Effect of melt processing conditions on the extent of exfoliation in organoclay-based nanocomposites," *Polymer*, vol. 42, no. 23, pp. 9513–9522, 2001.

[22] J. W. Gilman, A. B. Morgan, E. P. Giannelis, M. Wuthenow, and E. Manias, "Flammability and thermal stability studies of polymer layered-silicate (Clay) nanocomposites-II," in *Proceedings of the BCC Conference on Flame Retardancy*, pp. 1–11, 1999.

[23] P. G. Nahin and P. S. Backlund, Union Oil Company, United States patent no. 3, 084, 117, 1936.

[24] R. A. Vaia, H. Ishii, and E. P. Giannelis, "Synthesis and properties of two-dimensional nanostructures by direct intercalation of polymer melts in layered silicates," *Chemistry of Materials*, vol. 5, no. 12, pp. 1694–1696, 1993.

[25] R. A. Vaia, K. D. Jandt, E. J. Kramer, and E. P. Giannelis, "Microstructural evolution of melt intercalated polymer-organically modified layered silicates nanocomposites," *Chemistry of Materials*, vol. 8, no. 11, pp. 2628–2635, 1996.

[26] R. A. Vaia and E. P. Giannelis, "Lattice model of polymer melt intercalation in organically-modified layered silicates," *Macromolecules*, vol. 30, no. 25, pp. 7990–7999, 1997.

[27] M. Alexandre and P. Dubois, "Polymer-layered silicate nanocomposites: preparation, properties and uses of a new

class of materials," *Materials Science and Engineering R*, vol. 28, no. 1, pp. 1–63, 2000.

[28] S. Pavlidoua and C. D. Papaspyrides, "A review on polymer-layered silicate nanocomposites," *Progress in Polymer Science*, vol. 33, pp. 1119–1198, 2008.

[29] P. C. Lebaron, Z. Wang, and T. J. Pinnavaia, "Polymer-layered silicate nanocomposites: an overview," *Applied Clay Science*, vol. 15, no. 1-2, pp. 11–29, 1999.

[30] J. K. Kim, C. Hu, R. S. C. Woo, and M. L. Sham, "Rheology of confined polymer melts under shear flow: strong adsorption limit," *Composites Science and Technology*, vol. 65, p. 805, 2005.

[31] K. Chrissopoulou, I. Altintzi, S. H. Anastasiadis et al., "Controlling the miscibility of polyethylene/layered silicate nanocomposites by altering the polymer/surface interactions," *Polymer*, vol. 46, no. 26, pp. 12440–12451, 2005.

[32] G. Gorrasi, M. Tortora, V. Vittoria et al., "Vapor barrier properties of polycaprolactone montmorillonite nanocomposites: effect of clay dispersion," *Polymer*, vol. 44, no. 8, pp. 2271–2279, 2003.

[33] J. M. Yeh, H. Y. Huang, C. L. Chen, W. F. Su, and Y. H. Yu, "Siloxane-modified epoxy resin-clay nanocomposite coatings with advanced anticorrosive properties prepared by a solution dispersion approach," *Surface and Coatings Technology*, vol. 200, no. 8, pp. 2753–2763, 2006.

[34] J. Welti-Chanes, F. Vergara-Balderas, J. A. Guerrero-Beltrán, R. García Torres, and R. Villa-Rojas, "Métodos, criterios y modelación para la selección de películas plásticas en atmósferas modificadas," in *Segundo Simposio Internacional de Innovación y Desarrollo de Alimentos*, Montevideo, Uruguay, Septiembre 2005.

[35] S. Kenig, A. Ophir, O. Shepelev, and F. Weiner, "High barrier blow molded containers based on Nano Clay Composites," in *Proceedings of the Annual Technical Conference on the Society of Plastics Engineering*, San Francisco, Calif, USA, May 2001.

[36] M. C. Carrera, *Preparación y efecto de los nanocompuestos polímero-arcilla sobre las propiedades de barrera y mecánicas para polímeros hidrocarbonados y biodegradables [Ph.D. thesis]*, Universidad Nacional de Salta, Salta, Argentina, 2011.

[37] K. H. Wang, M. H. Choi, C. M. Koo, Y. S. Choi, and I. Chung, "Synthesis and characterization of maleated polyethylene/clay nanocomposites," *Journal of Polymer*, vol. 42, no. 24, pp. 9819–9826, 2001.

[38] H. A. Khonakdar, J. Morshedian, U. Wagenknecht, and S. H. Jafari, "An investigation of chemical crosslinking effect on properties of high-density polyethylene," *Polymer*, vol. 44, no. 15, pp. 4301–4309, 2003.

[39] C. Lotti, C. S. Isaac, M. C. Branciforti, R. M. V. Alves, S. Liberman, and R. E. S. Bretas, "Rheological, mechanical and transport properties of blown films of high density polyethylene nanocomposites," *European Polymer Journal*, vol. 44, no. 5, pp. 1346–1357, 2008.

[40] G. Choudalakis and A. D. Gotsis, "Permeability of polymer/clay nanocomposites: a review," *European Polymer Journal*, vol. 45, no. 4, pp. 967–984, 2009.